FLIGHT-DETERMINED BENEFITS OF INTEGRATED FLIGHT-PROPULSION CONTROL SYSTEMS

James F. Stewart
Frank W. Burcham, Jr.
Donald H. Gatlin
NASA Dryden Flight Research Facility
P.O. Box 273
Edwards, California, USA

Abstract

Over the last two decades, NASA has conducted several flight research experiments in integrated flight-propulsion control. Benefits have included improved maneuverability; increased thrust, range, and survivability; reduced fuel consumption; and reduced maintenance. These flight programs were flown at NASA Dryden Flight Research Facility, with NASA Lewis and Langley Research Centers and the Department of Defense. This paper presents the basic concepts for control integration, examples of implementation, and benefits.

The F-111E experiment integrated the engine and inlet control systems. The YF-12C incorporated an integrated control system involving the inlet, autopilot, autothrottle, airdata, navigation, and stability augmentation systems. The F-15 research involved integration of the engine, flight, and inlet control systems. Further extension of the integration included real-time, onboard optimization of engine, inlet, and flight control variables; a self-repairing flight control system; and an engines-only control concept for emergency control. The F-18A aircraft incorporated thrust vectoring integrated with the flight control system to provide enhanced maneuvering at high angles of attack. The flight research programs and the resulting benefits for each are described, but particular emphasis is given to the F-15 research.

Nomenclature

ADECS	adaptive digital engine control system
CAS	control augmentation system
DEEC	digital electronic engine control
DEFCS	digital electronic flight control system
DFCC	digital flight control computer
EEL	extended engine life
EGE	effective gain estimator
EMD	engine model derivative
EPR	engine pressure ratio
FDIE	fault detection isolation and estimation
FTIT	fan turbine inlet temperature
HARV	High Alpha Research Vehicle
HIDEC	highly integrated digital electronic control
HUD	heads-up display
INS	inertial navigation system
IPCS	integrated propulsion control system
NASA	National Aeronautics and Space Administration
NPR	nozzle pressure ratio
P_{amb}	ambient pressure, lb/in^2
PROTECT	propulsive techniques for emergency control
PSC	performance seeking control
SIDC	system impairment detection and classification
SRFCS	self-repairing flight control system
TSFC	thrust specific fuel consumption
USAF	United States Air Force
α	angle of attack, deg
β	angle of sideslip, deg
δv	vane deflection angle

Introduction

The integration of propulsion control systems and propulsion-flight control systems has been shown to significantly improve airplane performance parameters such as thrust, range, and rate of climb. When systems are not integrated, each system must be able to operate in a worst-case combination with the other systems, and large operating margins are required. Integration allows these margins to be reduced when the full margins are not required, resulting in higher thrust, lower fuel flow or greater maneuverability or range, and better safety and reliability. Integration control laws are developed in an off-line process and stored in an onboard computer for implementation. System performance was further improved by real-time optimization used in place of the *a priori* or preprogrammed optimization. The real-time approach is much more challenging to develop and implement; but because it can adapt to flight conditions, it may achieve higher levels of performance.

To study the problems of integration and to determine the benefits of integration in the actual flight environment, NASA Dryden has conducted flight research over the past two decades. In the mid-1970's, propulsion system digital control and control integration were developed and demonstrated in the Integrated Propulsion Control System (IPCS) Program (Ref. 1), a joint United States Air Force (USAF) and NASA program flown on an F-111E airplane. The flight demonstration clearly showed the benefits of digital control and control integration.

In the late 1970's, a digital cooperative control system was flown on the NASA YF-12C airplane (Ref. 2). This system integrated the inlet control, autothrottle, airdata, and navigation functions, and it dramatically improved flightpath control and range, though the integration was not optimized. This technology was transitioned into production when the concept was implemented on the SR-71 fleet.

In the early 1980's, NASA transitioned integrated controls research to the F-15 airplane. First, the digital electronic engine control (DEEC) was flight-tested (Ref. 3). Later, the engine control was integrated with the flight control system in the Highly Integrated Digital Electronic Control (HIDEC) Program (Ref. 4). This program demonstrated significant improvements in thrust, fuel consumption, and engine life. Further extension of the integration to include real-time, onboard optimization of engine, inlet, and flight control variables (performance seeking control (PSC)) was also accomplished (Ref. 5). Integration also made it possible to develop a self-repairing flight control system (SRFCS) on the F-15 (Ref. 6), which has been successfully tested. A propulsion-only flight control system, which uses the engines for emergency flight control, was also developed and tested (Ref. 7).

Finally, the design of the F-18A High Alpha Research Vehicle (HARV) integrated a thrust vectoring system with the flight control system. This has significantly improved high-angle-of-attack maneuverability.

This paper presents an overview of the integration research programs conducted on the F-111E, YF-12C, F-15, and F-18A airplanes. Figure 1 depicts the chronological order of each integrated control flight research program. Descriptions and benefits of each program are discussed, but the F-15 research is given the most emphasis based on the relative contributions made.

Integrated Propulsion Control System (F-111E)

The first IPCS was installed on an F-111E (Ref. 1), a long-range tactical fighter-bomber airplane. It features variable sweep wings, a crew of two, and a maximum Mach capability of 2.5. It is powered by two TF30 afterburning turbofan engines fed by variable-geometry external compression inlets.

The F-111E engine and inlet are normally equipped with independent hydromechanical control systems. For the IPCS program, a full-authority digital engine control system was developed and implemented in an onboard research computer. Either a digital implementation of standard hydromechanical control or a new digital control mode could be selected. The TF30 engine digital controller was also integrated with the control of the variable geometry external compression inlet. Significant performance benefits included stall-free operation, faster throttle response, increased thrust, and increased range at Mach number 1.8. Figure 2 summarizes these results.

YF-12C Flight Research

Airplane Description

As mentioned previously, NASA conducted a research program on flight control systems and propulsion system–flight control interactions on the YF-12C airplane (Ref. 2). The YF-12C airplane (Fig. 3) was a twin-engine, delta-winged airplane designed for long-range cruise at Mach 3.2+ and altitudes above 85,000 ft. Two nacelle-mounted, all movable vertical tails provided directional stability and control. Two elevons on each wing, one inboard and one outboard of each nacelle, performed the combined function of elevators and ailerons. The airplane was normally operated with the stability augmentation system engaged to provide artificial stability in pitch and yaw and to provide damping in pitch, yaw, and roll.

The airplane had two axisymmetric, variable geometry, mixed compression inlets that supplied air to two J58 engines. Each inlet had a translating spike and forward bypass doors. An automatic inlet control system varied the spike and bypass door positions. The spike position was scheduled with flight conditions to set the throat Mach number. A closed-loop system controlled the bypass doors as a function of flight conditions and duct pressure. The system optimally positioned the terminal shock wave, subject to inlet stability constraints.

High-speed supersonic cruise at Mach numbers greater than 2.5 and at altitudes above 70,000 ft highlighted many new airframe–propulsion system interdisciplinary problems that impacted efficient aircraft operation. Early flight research results showed strong interactions between control systems. For example, at high speed, the bypass doors were as effective as the rudders in providing yawing moment. With the stability augmentation system off, the automatic inlet control system operation destabilized the yaw axis. The phugoid mode was unstable with the automatic inlet control operating. The altitude-hold autopilot was also unstable in some flight conditions. Integration of subsystems was seen as an effective way to take advantage of favorable interactions and to minimize unfavorable interactions.

Integrated Controller Design

Studies by NASA have indicated that problems such as those discussed earlier may be solved by developing an integrated–cooperative control system for supersonic cruise vehicles. Other benefits that may be realized are improved

inlet stability and reduced engine temperatures, propulsion system drag, trim drag, weight, and control surface size.

Studies were initiated by NASA to develop integrated control concepts and thereby validate some of these benefits. One NASA-supported design study developed an integrated lateral-directional augmentation system using inlet controls. This system could be based on the previously discussed airframe–propulsion system interactions and force-and-moment measurements.

The results of the study indicated that incorporation of inlet control geometry into the lateral-directional stability augmentation was effective in increasing dutch roll damping. This incorporation was accomplished while still maintaining inlet unstart protection, even in moderate to heavy turbulence. The study also showed that using the propulsion system to augment the flight controls reduced the takeoff gross weight of a supersonic cruise aircraft up to 7 percent.

Flight Demonstration of a Cooperative Control System

To demonstrate the above concepts, a cooperative digital control system replaced several separate analog–mechanical control systems of the NASA YF-12C research airplane. All functions shown on Fig. 4 (inlet control, autopilot, autothrottle, airdata, and navigation) were performed in a single computer. The central digital computer control provided more accurate and faster response computations. The improved altitude- and Mach-hold autopilot logic was incorporated. Airdata computations were improved, and lag compensation was applied. In addition, more precise inlet control was obtained with the digital system while inlet stability margins were reduced. The overall result of the flight research was that range was increased by 5 percent. Altitude control capability was improved by an order of magnitude as compared with manual control.

Implementation on the SR-71 Fleet

Based on the success of the digital flight–propulsion control system on the YF-12C, the SR-71 (the production version of the YF-12C) fleet incorporated the cooperative control system concepts as part of a major avionics upgrade. In fleet use, this system realized range improvements of 7 percent and eliminated the occurrence of inlet unstarts. Thus, the flight demonstration served to speed the transition of the technology developed in the YF-12C flight–propulsion control research to the operational SR-71 fleet.

F-15 HIDEC Flight Research

Airplane Description

The NASA F-15 HIDEC Flight Research Aircraft is a national facility for conducting integrated flight-propulsion control research. It is a single-seat, high-performance fighter with excellent transonic maneuverability and a maximum Mach capability of 2.5. Two afterburning turbofan engines power the F-15, and it has a high-mounted swept-back wing, twin vertical stabilizers, and large horizontal stabilizers. The engine inlets are the two-dimensional external compression type with three ramps and feature variable capture area. Figure 5 shows a three-view drawing of the F-15 aircraft. The airplane is almost 64 ft long and has a wingspan of nearly 43 ft.

The configuration of the NASA F-15 enhances its flexibility for research, since it does not have most of the weapons systems equipment that is part of the standard F-15 aircraft. Absent are the radar, gun, missiles, and weapons systems avionics. This provides a large volume of space for experiments and instrumentation.

Flight Control System

The standard F-15 airplane is equipped with a mechanical flight control system that provides control of the ailerons, rudders, and stabilizers. An analog electronic control augmentation system (CAS) operates in all three axes.

For the NASA F-15 airplane, a digital electronic flight control system (DEFCS) augments the standard flight control system. The DEFCS replaces the analog CAS. It is a dual-channel, fail-safe system programmed in Pascal. The Military Standard 1553B (Ref. 8) data bus input-output capability and the unused capacity in the DEFCS computers may be used for other functions.

Engine Control System

The standard F100-PW-100 engines (Pratt & Whitney, West Palm Beach, FL) have a hydromechanical control and a supervisory electronic engine control. The F100 engine model derivative (EMD) engines have DEEC systems. The DEEC is a full-authority, single-channel control with a simple hydromechanical secondary control. A universal asynchronous receiver-transmitter data bus provides input-output capability. These engine controls may communicate with the DEFCS for integrated control research.

Inlet Control System

A digital control system positions the three inlet variables. These inlet controllers were modified to accept bias signals for the inlet cowl and ramps from the DEFCS, making integrated inlet control research possible.

Avionics

The F-15 avionics system has evolved over the years as a result of integrated controls research programs. Figure 6 shows a recent system architecture, and Fig. 7 depicts the aircraft configuration. Three data busses are used to communicate between the various components, and a data bus interface and control unit ties these busses together.

On the Military Standard 1553 bus are the DEFCS, the NASA data system, an uplink telemetry system that receives information transmitted from a ground-based computer and a general-purpose digital computer. This general-purpose computer uses 32-bit words and has a throughput of approximately 2.5 million instructions/sec and a memory of 2 Mbytes. This computer may be programmed in high-order languages such as Ada, FORTRAN, and Pascal. It has been used for the PSC subsonic flight research.

The standard F-15 (H009) data bus communicates with the inertial measuring unit, the attitude and heading reference set, a horizontal situation indicator, an airdata computer, a central computer, and a cockpit navigation control indicator. The DEECs installed on both engines constitute the remaining part of the avionics system. Their universal asynchronous receiver-transmitter data bus communicates with the aircraft through the data bus interface and control unit. The NASA F-15 aircraft, configured with this avionics system, provides a uniquely capable and flexible system for controls integration research.

Integrated Flight Propulsion Control Modes

The pilot carried out the only integration of aircraft–engine controls in the original F-15 by trying to optimize throttle and stick commands for a given mission. Trim control and feedback compensation were carried out by separate flight, inlet, and engine controllers without benefit of shared information.

The designers were aware of the airflow demands of the engine and designed the F-15 variable inlet geometry schedules accordingly. The designers of the DEEC knew what pressure distortion levels were encountered behind the F-15 inlet; engine control laws were produced with sufficient stability margin to ensure stall-free engine operation at the worst levels of distortion. But because the subsystems were not designed to communicate in flight, performance compromises were unavoidable.

Adaptive Digital Engine Control System

Figure 8 depicts the integration of the engine control system to the flight control system. In using ADECS, additional thrust was obtained at intermediate and above intermediate power settings by decreasing the nozzle throat area to increase the engine pressure ratio (EPR). This occurs at near constant airflow. The EPR is increased until the fan turbine inlet temperature (FTIT) limit is approached. Thrust is increased at the expense of reduced engine stall margin.

Substantial stall margin is built into engine control schedules to accommodate the distortion produced at high angles of attack or high sideslip angles. In the ADECS at EPR mode, some of the stall margin reserved for extreme inlet distortion is used to increase thrust in regions of low distortion. As flight conditions produce high inlet distortion, the amount of EPR uptrim is reduced to restore stall margin. Figure 9 shows a typical stability audit with and without EPR uptrim. Additional information on stability audits and definition of the amount of stall margin available are found in Ref. 4.

The EPR uptrim control law is implemented in the digital flight control computer (DFCC). When the predicted angle of attack (α) and sideslip angle (β) are moderate, the controller issues an EPR command to the engine causing the engine to operate close to the stall line. The DFCC uses airframe pitch, roll, and yaw rates and normal, lateral, and axial accelerations to predict angles of attack and sideslip. As these predicted angles become large, the controller decreases the uptrim signal to ensure stall-free engine operation. Details of the EPR uptrim logic are given in Ref. 4.

The ADECS also provides a constant-thrust or extended engine life (EEL) mode that improves the engine thrust-specific fuel consumption (TSFC) and increases engine life by reducing turbine temperature. This EEL mode increases EPR while reducing engine airflow to maintain constant thrust for a given power setting. Figure 10 illustrates this mode.

Flight Results

Figure 11 indicates the improvements in thrust for intermediate power at various altitudes. These improvements range from approximately 8 percent at 10,000 ft to 10.5 percent at 30,000 ft. If the engine is uptrimmed using the excess stall margin while thrust is held constant, TSFC can be reduced as shown in Fig. 12. At 30,000 ft, Mach 0.6 and maximum power, a 16-percent reduction in TSFC was obtained. This compares well with the predicted value of 17 percent. More details of predicted versus actual results can be found in Ref. 9.

The EEL mode was shown to reduce engine turbine temperature up to 80 °F. Figure 13 shows this reduction in temperature. This has been predicted by the engine manufacturer to be equivalent to reducing high-pressure turbine wear rate by 50 percent at high-power settings. Over a typical mission profile, this results in 10- to 15-percent increased turbine life.

The ADECS test results proved that substantial gains in excess thrust (thrust minus drag) for increased performance, or reduction in FTIT for extended engine life, can be realized through integrated controls.

Performance Seeking Control

Personnel at NASA anticipated that additional benefits could be realized by replacing the ADECS schedules, which are based on a normal engine, with a model-based

control algorithm that adapts to engine variations. The PSC was designed to develop such an adaptive, integrated flight–propulsion control algorithm and to demonstrate this control technique in flight.

The PSC onboard adaptive real-time optimization algorithm has three modes: the maximum thrust mode, which maximizes excess thrust (thrust minus drag) during accelerations, climbs, and dashes; the minimum fuel mode, which minimizes fuel consumption during aircraft cruise; and the minimum FTIT mode, which extends engine life by reducing FTIT.

The standard engine sensors provide input information to a Kalman filter, which estimates engine component deviations to account for other than nominal engine performance. These component deviations represent changes in fan low-pressure turbine efficiency, fan airflow, compressor high-pressure turbine efficiency, core airflow, and core turbine area. The deviations are estimated within the accuracy of the Kalman filter and its inputs (Ref. 10).

The component deviation estimates are used to match the onboard engine model to the operating characteristics of the actual engine. The engine model, updated with the current engine component deviations, is combined with an engine exhaust nozzle model that calculates the internal nozzle performance and external boattail drag as a function of engine and flight condition. An inlet-trim drag model represents the performance of the inlet first ramp on inlet pressure recovery, drag, and pitching moment, and the associated change in the horizontal tail position and its associated trim drag. The inlet third ramp effects on inlet drag and recovery are also modeled. This model is assumed to be time invariant.

These models are simpler than the off-line simulation used in ADECS. The PSC approach has the advantage, however, of tuning these models in flight. During the current PSC research, only the engine model is required to change with time to match the actual system operating condition.

The PSC uses a linear-programming algorithm to optimize the performance objectives. The PSC approach performs a series of constrained local linear-programming optimizations to converge to a global optimization. The outputs of the optimization are two inlet variables (the cowl position and the third ramp position), the nozzle area, engine fan and compressor variable vane positions, core and afterburner fuel flow, fan airflow, and fan speed as illustrated in Fig. 14. These optimized commands are sent to the inlet controller and to the engine controller. A detailed description of the model, update logic, and the optimization process can be found in Ref. 11.

Flight Results

The PSC algorithm was flight-tested throughout the subsonic envelope for both degraded and refurbished (overhauled) engines. Supersonic flight tests will be initiated in late 1992. Results have shown that PSC produces significant thrust increases at key flight conditions (Fig. 15). Thrust increases of up to 15 percent were obtained on a refurbished engine. A 9-percent improvement was obtained in the degraded engine.

The PSC extended life mode shows a turbine temperature decrease of more than 160 °F at 0.9 Mach, 15,000 ft, military power, while holding constant thrust (Fig. 16). Data with and without the engine model update logic (Kalman filter) show that using the component deviation parameters improves the optimization process over optimization with a standard engine model. This can be seen from the additional decrease in engine turbine temperature of more than 60 °F.

The engine manufacturer estimates that at high-power settings, the engine high-pressure turbine wear rate is reduced by 50 percent for a 70 to 80 °F temperature reduction. Therefore, significant engine life extension can be obtained using PSC. In addition to the reduced operating turbine temperature, fuel flow was reduced 2 percent while holding constant thrust.

Self-Repairing Flight Control System Program

The F-15 HIDEC program, sponsored by the USAF, has developed, implemented, and flight-tested a SRFCS. This program includes control reconfiguration, a heads-up display (HUD) positive pilot alert system, and knowledge-based maintenance diagnostics.

The SRFCS program approach exploits the inherent control redundancies of advanced aircraft by fully using its multiple control effectors and their secondary aerodynamic characteristics. This is accomplished by reconfiguration, after control effector failures, to allow control substitution by the remaining effectors. Instead of using massive redundant hardware on each effector to achieve fault tolerance and reliability, the redundant elements become the aerodynamic forces and moments produced by the other control effectors. The necessary forces and moments are generated by the alternate control surfaces to provide the required aircraft motion.

In today's fighter and transport-commercial aircraft, the control systems have the power and surface displacement to maneuver the aircraft in a very large flight envelope, with surplus control capacity available from each control surface. If failure or loss of a control surface occurs, the SRFCS uses this surplus capacity by reconfiguring control commands to

the remaining control surfaces, and thus preserve the maneuvering response.

Reconfiguration is one of the few technologies that holds promise to meet the availability and survivability requirements for aircraft in a hostile environment, while minimizing the complexity and costs of the system. Knowledge-based diagnostics can provide timely and accurate fault isolation for maintenance and reduce the unnecessary removal of nonfailed equipment.

The technologies demonstrated in this joint NASA and USAF flight program include control reconfiguration, fault detection and isolation, positive pilot alert, and maintenance diagnostics. Figure 17 illustrates how the technologies were integrated with the F-15 HIDEC aircraft. Details of each technology area and the SRFCS process can be found in Ref. 6. Each area is highlighted as follows:

Control Mixer Reconfiguration Strategy. The core element of the reconfiguration strategy was the control mixer. The mixer accepted the outputs of a preexisting set of control laws designed for an unimpaired airplane and reallocated these outputs to the surviving effectors of an impaired airplane.

Fault Detection Isolation and Estimation (FDIE). Fault isolation was accomplished by hypothesis testing through sequential probability ratio tests, a scheme successfully used on the NASA F-8 digital fly-by-wire analytic redundancy management experiment.

Positive Pilot Alert. An integral part of the reconfiguration philosophy was the presentation in the HUD of the surviving flight control system status information to the pilot, including a situation assessment of the existing performance limits of the damaged aircraft.

Maintenance Diagnostics. In addition to the reconfiguration, the SRFCS had an expert system capability that could detect and isolate system component failures occurring in routine aircraft use. These onboard diagnostics were adept at finding intermittent faults that happened only in flight and relating them to casual events such as maneuver action, cooling temperature, pilot input sequence, or other fact relationships that may be impossible to reconstruct in postflight maintenance troubleshooting.

Implementation

The SRFCS tested was capable of emulating an impairment and reconfiguration after detection of the impairment. The SRFCS impairment failure modes could be selected by the pilot and flown to assess the performance of the F-15 aircraft with and without the impairment. Figure 18 is a block diagram of the F-15 SRFCS implementation, which includes both standard mechanical and electronic CAS. The F-15 HIDEC CAS serves to provide stability augmentation and command response enhancement through control laws implemented in a dual-channel DFCC.

The baseline mode was unchanged until an impairment was introduced. Two SRFCS commands, shown in Fig. 18, were added to the F-15 HIDEC CAS servo controller commands. The first command forced the control system to represent failure conditions. (This software was for flight test only.) The second command added a reconfiguration correction to each control surface servo controller. Additional details of the implementation in the F-15 HIDEC aircraft can be found in Ref. 12.

The flight test aircraft was configured with three impairments that were selectable by the pilot. All impairments affected the right horizontal stabilator. The impairments were activated with software commands to the stabilator servo actuator to accurately represent the desired failure (Fig. 18). The commands negated the mechanical system inputs and set the stabilator for the desired impairment. Once the failure type was selected and activated by the pilot, it remained active throughout the fault detection sequence and pilot evaluation of the reconfigured airplane. Both the failure and the correction commands disappeared upon pilot deactivation of the reconfiguration test mode through a switch on the control stick. Three types of failure modes were mechanized and fight-tested:

1. Locked at trim - representing hydraulic or mechanical failure.

2. Locked at an offset position - representing a failure caused by hydraulic or mechanical jam. Values up to 6° offset locked position could be flown.

3. Partial surface loss - representing a portion of the right stabilator missing because of midair collision or battle damage of 50-, 80-, and 100-percent surface loss.

Flight Test Process

Figure 19 shows the flight envelope used for SRFCS development. The system was developed for the design envelope, but it was also tested in the pilot maneuver envelope. The pilot could select various impairments and SRFCS test modes. The following table displays the conditions flown: (a) impairments of the right stabilator, (b) the maneuver sequence, and (c) the SRFCS subroutine or test mode that could be selected by the pilot. Tests were also conducted on the maintenance diagnostics system using maneuver sequences designed to trigger the fault scenarios shown in Fig. 20.

Test conditions.

(a) Right-stabilator impairment.
Locked at trim
Locked at +2°
Locked at +4°
Locked at +6°
80-percent missing span
100-percent missing span
50-percent missing span
(b) Test maneuvers.
Pitch and roll stick doublets
Pushover and pullup
3-*g* windup turn
3-*g* bank-to-bank roll
(c) Configuration.
No impairment
Impairment
Impairment with fault detection
Impairment with effector estimator
Impairment with reconfiguration mixer
Impairment with complete reconfiguration sequence

Flight Results

Figure 21 shows the summary results of the FDIE. The FDIE performance was directly related to the onboard simulation model fidelity.

The flight performance of the reconfiguration mixer was judged satisfactory by the NASA evaluation pilots, with the largest effects occurring for the 6° locked-stabilator impairments. This impairment required large stick offsets just to maintain level flight, while the reconfigured system permitted the pilot to control with normal stick position. Figure 22 is an example of the stick position change. The indication was that after reconfiguration, no offset was required to control the reconfigured aircraft.

Figure 23 shows an example of the F-15 test aircraft SRFCS software performing the reconfiguration for a battle-damaged right stabilator missing 80 percent of its span. The fault was detected as the pilot initiated a bank maneuver, and the reconfiguration engaged 0.35 sec later. The bank response was maintained very close to the undamaged F-15 response. Additional results of the SRFCS flight test program can be found in Refs. 6 and 12.

Planned Research Using Propulsion-Only Controls Technology

The SRFCS is flight-proven technology for practical application of new flight control systems which will greatly increase the survivability of combat aircraft and enhance survivability of combat aircraft and commercial aircraft. Part of the NASA Dryden research investigation was undertaken to develop methods for emergency control for multisurface failures and for the extreme case when most or all of the flight control system became inoperative. For multiengined aircraft the research led to techniques that use the throttles for emergency controls. This research has shown that to some degree, most multiengined aircraft can be controlled by a closed-loop, propulsion-only flight control system. This breakthrough technology for emergency control will be flight-demonstrated on the NASA F-15 HIDEC aircraft in late 1992.

The augmented control system has been implemented on the NASA Dryden F-15 simulator. The propulsion-only control technique has two important features:

1. Flight controllers such as a stick or autopilot type pitch and bank angle control knobs can be used to control the aircraft.

2. The system uses feedback of key pitch and roll parameters to stabilize and accurately control the flightpath.

Figure 24 shows a block diagram of the augmented control system. In the pitch axis, flightpath angle and pitch rate feedback provide phugoid damping to stabilize the system. In the roll axis, the roll rate, bank angle, and sideslip parameters are used as required to obtain the satisfactory bank angle control. Details of the F-15 propulsion-only flight controls can be found in Ref. 7.

Simulation results, Fig. 25, have shown that precise control capability was greatly enhanced using the closed-loop (augmented) control system. Simulation results indicate that even inexperienced pilots were able to make acceptable emergency landings on the first try. Details of the simulation results for the F-15 and commercial aircraft can be found in Ref. 13.

Integrated Propulsion and Aerodynamic Controls (F-18A)

The HARV is an F-18A modified to incorporate thrust vectoring vanes for propulsive control augmentation permitting maneuvering flight at angles of attack up to 70°. Figure 26 shows the aircraft with the vectoring system installed. The mechanical vectoring system consists of three airframe mounted vanes per engine. The divergent nozzle of the F-404–GE400 engines has been removed to reduce the bending moment imparted to the airframe by the vane supports. Figure 27 shows vectoring capability. The vanes are commanded by experimental control laws running in a research flight control system using a 1750A processor embedded within the production F-18A flight control computers. The research flight control system operates only between 15,000- and 35,000-ft altitude and below 0.7 Mach, which significantly reduces the complexity and size of the control laws. It is a fail-safe system, reverting to the F-18A

control system in the event of system- or pilot-detected research flight control system failures. The control laws are an alpha command in pitch and a wind axis roll rate command laterally with both thrust and aerodynamic controls responding initially to pilot commands. The thrust vanes are washed out if the aerodynamic surfaces are sufficiently powerful. The rudder pedals command sideslip. When engaged, the system requires no unusual pilot technique.

Flight experience with the system has been successful to date. The envelope expansion tests demonstrated stabilized flight at $\alpha = 70°$, 1-g velocity vector rolls at $\alpha = 65°$, and stall-free engine operation. The aerodynamically controlled F-18A has very limited rolling capability above $\alpha = 35°$ and experiences severe wing rock for angles of attack between 35° and 45°. The addition of vectoring has eliminated the wing rock and provides significant rolling performance through $\alpha = 65°$.

Concluding Remarks

The use of digital control systems and their ability to share information and act on that shared information in an intelligent manner allow for better control of the individual systems and the overall aircraft. This has resulted in significant performance benefits as highlighted in this paper and the referenced research. The potential payoff for integrated technologies has barely begun. The implications of integrated technologies on future aircraft design are only now starting to be understood. The use of these and other integrated control systems on the overall aircraft configuration, and the synergistic effect of integrated technologies in new designs, will allow major improvements in performance, reliability, and survivability of future aircraft.

References

[1]Burcham, Frank W., Jr. and Batterton, Peter G., "Flight Experience with a Digital Integrated Propulsion Control System on an F-111E Airplane," AIAA-76-653, July 1976.

[2]Burcham, F., Gilyard, G., and Myers, L., "Propulsion System - Flight Control Integration - Flight Evaluation and Technology Transition," AIAA-90-2280, July 1990.

[3]Burcham, F.W., Jr., Myers, L.P., and Walsh, K.R., "Flight Evaluation of a Digital Electronic Engine Control in an F-15 Airplane," *J. Aircraft*, vol. 22, no. 12, Dec. 1985, pp. 1072–1078.

[4]Myers, L.P. and Walsh, K.R., "Performance Improvements of an F-15 Airplane with an Integrated Engine-Flight Control System," *J. Aircraft*, vol. 28, no. 12, Dec. 1991, pp. 812–817.

[5]Lambert, H.H., Gilyard, G.B., Chisholm, J.D., and Kerr, L.J., *Preliminary Flight Evaluation of an Engine Performance Optimization Algorithm*, NASA TM-4328, June 1991. (Available also as AIAA-91-1998.)

[6]Urnes, J.M., Stewart, J., and Eslinger, R., "Flight Demonstration of a Self Repairing Flight Control System in a NASA F-15 Fighter Aircraft," AGARD Guidance and Control Panel 49th Symposium, Toulouse, France, Oct. 1989.

[7]Burcham, Frank W., Jr. and Fullerton, C. Gordon, *Controlling Crippled Aircraft–With Throttles*, NASA TM-104238, Sept. 1991.

[8]USAF, MIL-STD-1553B, Digital Time Division Command/Response Multiplex Data Bus, Sept. 8, 1986. Available from Aeronautical Space Division, AFSC, Wright-Patterson AFB, Ohio.

[9]Myers, Lawrence P. and Burcham, Frank W., Jr., "Preliminary Flight Test Results of the F100 EMD Engine in an F-15 Airplane," AIAA-84-1332, June 1984.

[10]Orme, John S. and Gilyard, Glenn B., "Subsonic Flight Test Evaluation of a Propulsion System Parameter Estimation Process for the F100 Engine," AIAA-92-3745, July 1992.

[11]R.H. Smith, Chisholm, J.D., and J.F. Stewart, "Optimizing Aircraft Performance with Adaptive, Integrated Flight/Propulsion Control," ASME Gas Turbine and Aeroengine Congress and Exposition, June 11–14, 1990, Brussels, Belgium.

[12]Stewart, James F. and Shuck, Thomas L., "Flight-Testing of the Self-Repairing Flight Control System Using the F-15 Highly Integrated Digital Electronic Control Flight Research Facility," AIAA-90-1321, May 1990.

[13]Gilyard, Glenn B., Conley, Joseph L., Le, Jeanette, and Burcham, Frank W., Jr., *A Simulation Evaluation of a Four-Engine Jet Transport Using Engine Thrust Modulation for Flightpath Control*, NASA TM-4324, Sept. 1991. (Available also as AIAA-91-2223.)

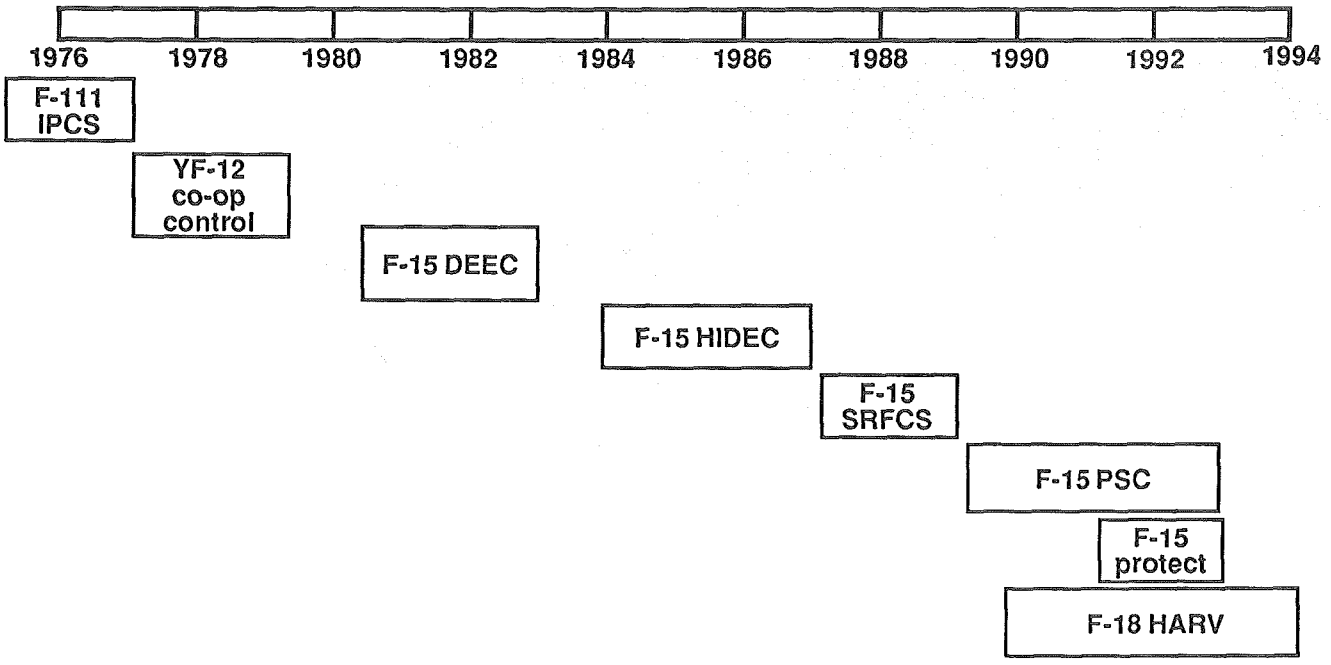

Figure 1. Integrated control flight research programs.

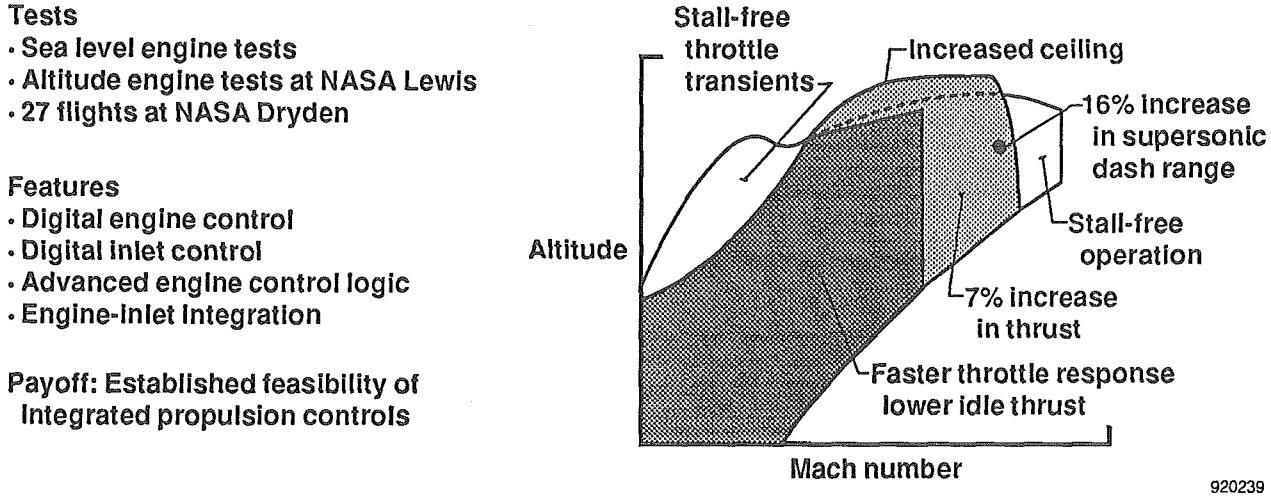

Figure 2. Results of the F-111E integrated propulsion control system.

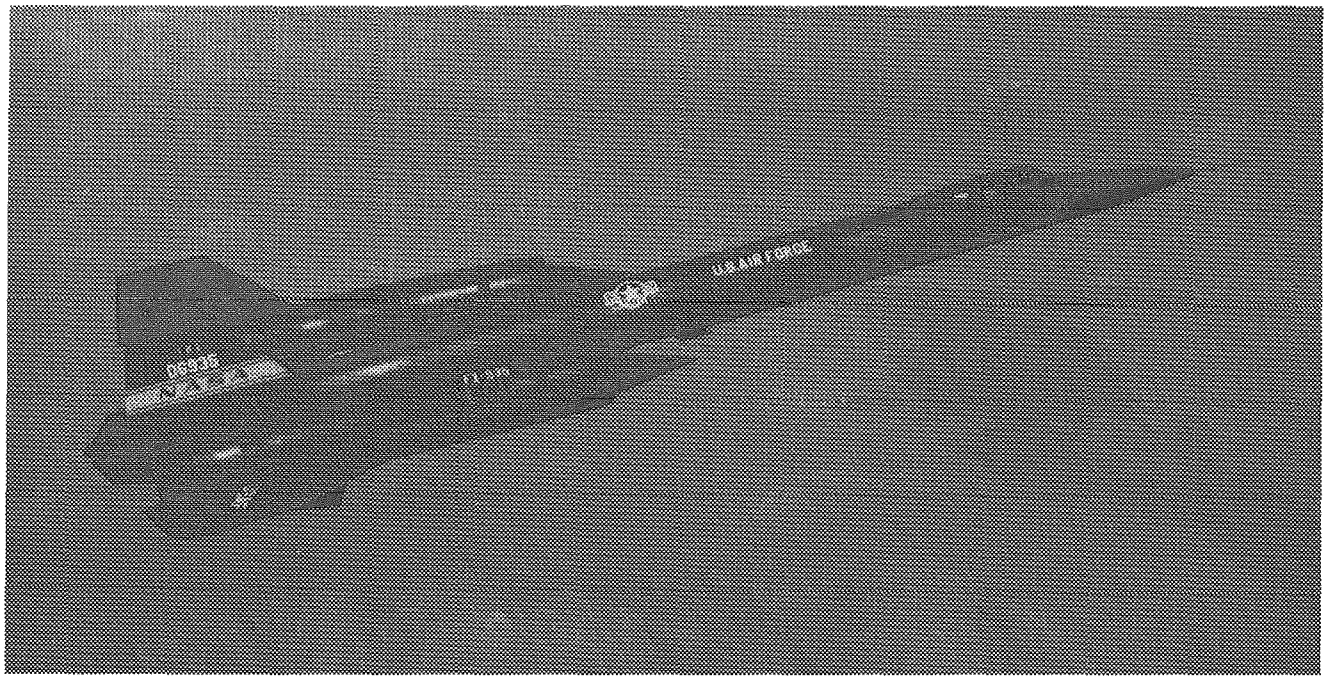

ECN 2704

Figure 3. YF-12C research aircraft.

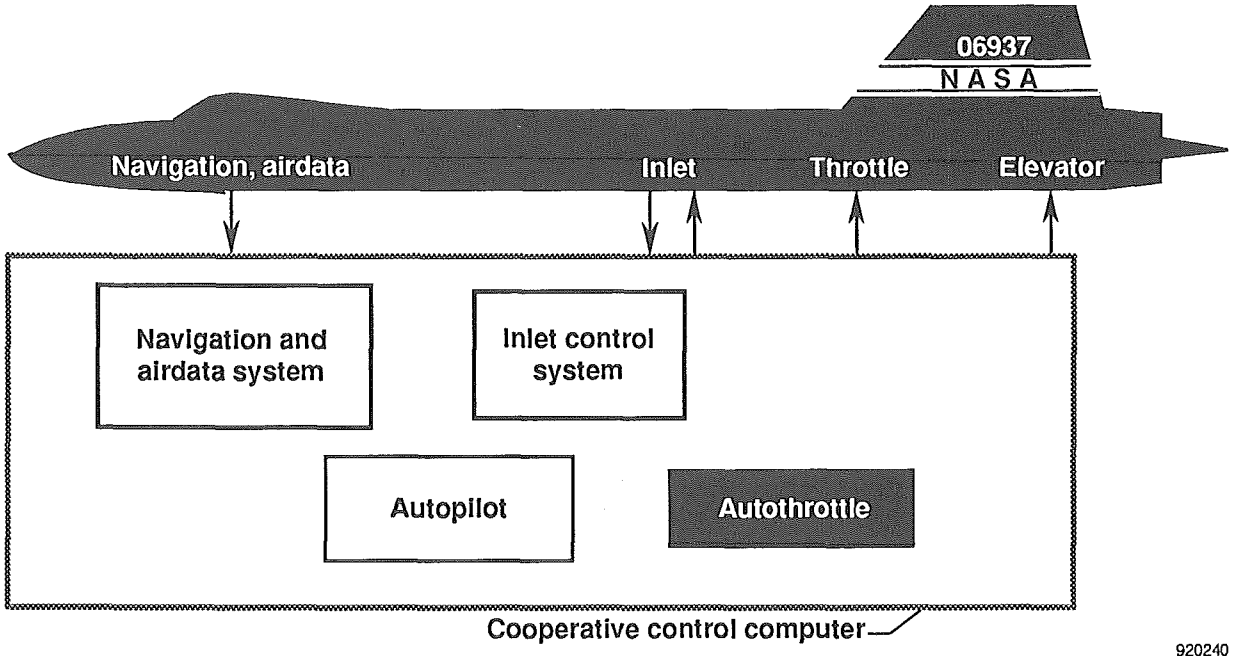

Figure 4. YF-12C cooperative control system.

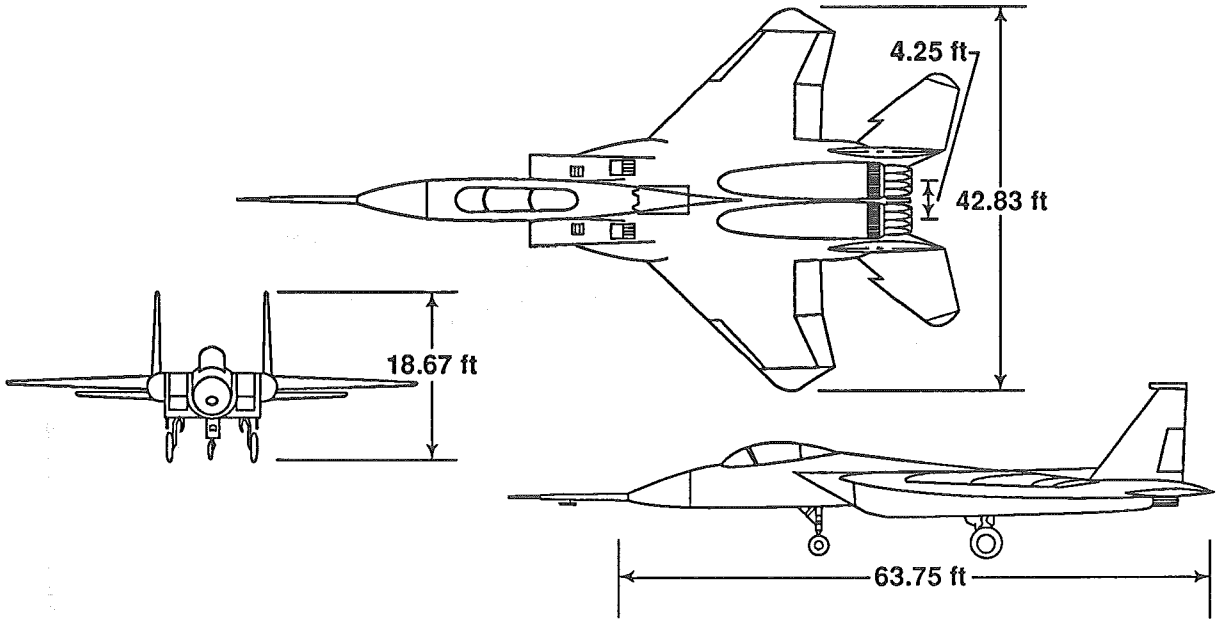

Figure 5. NASA F-15 HIDEC flight research aircraft.

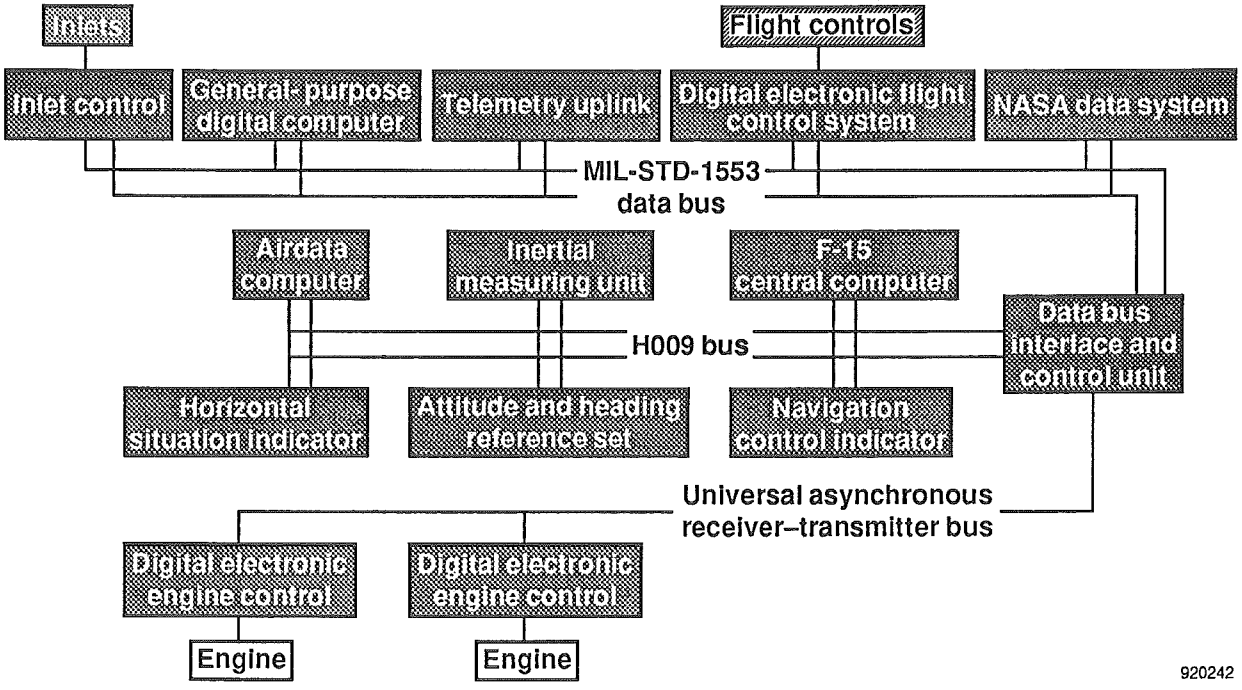

Figure 6. F-15 avionics system architecture.

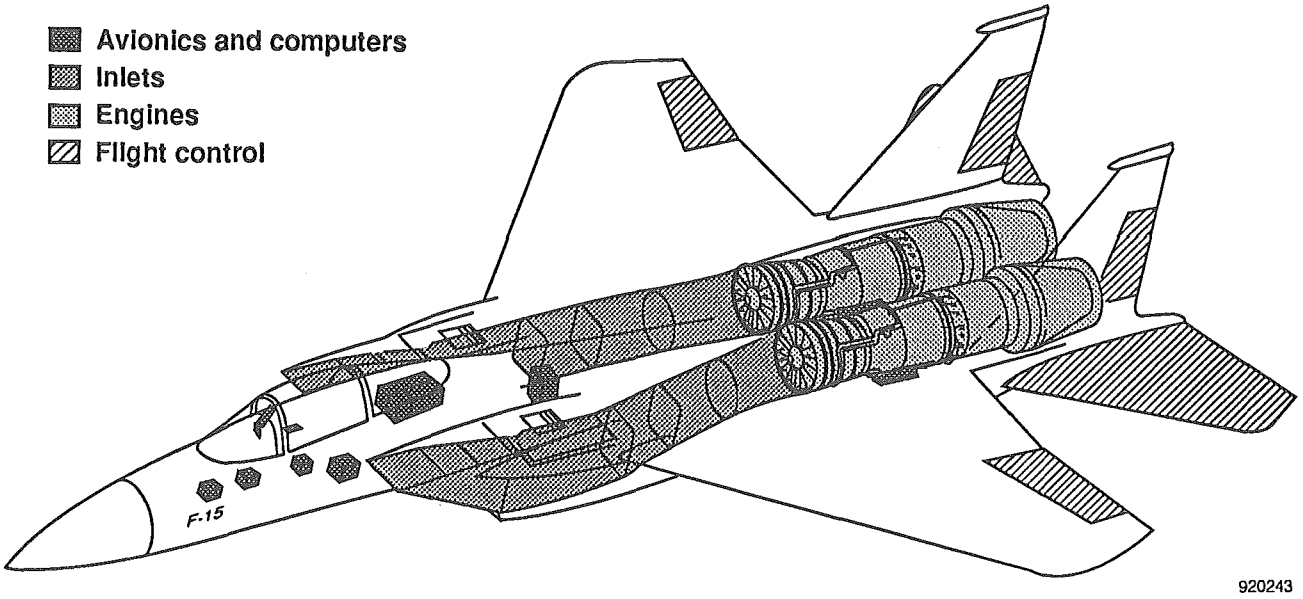

Figure 7. F-15 avionics system configuration.

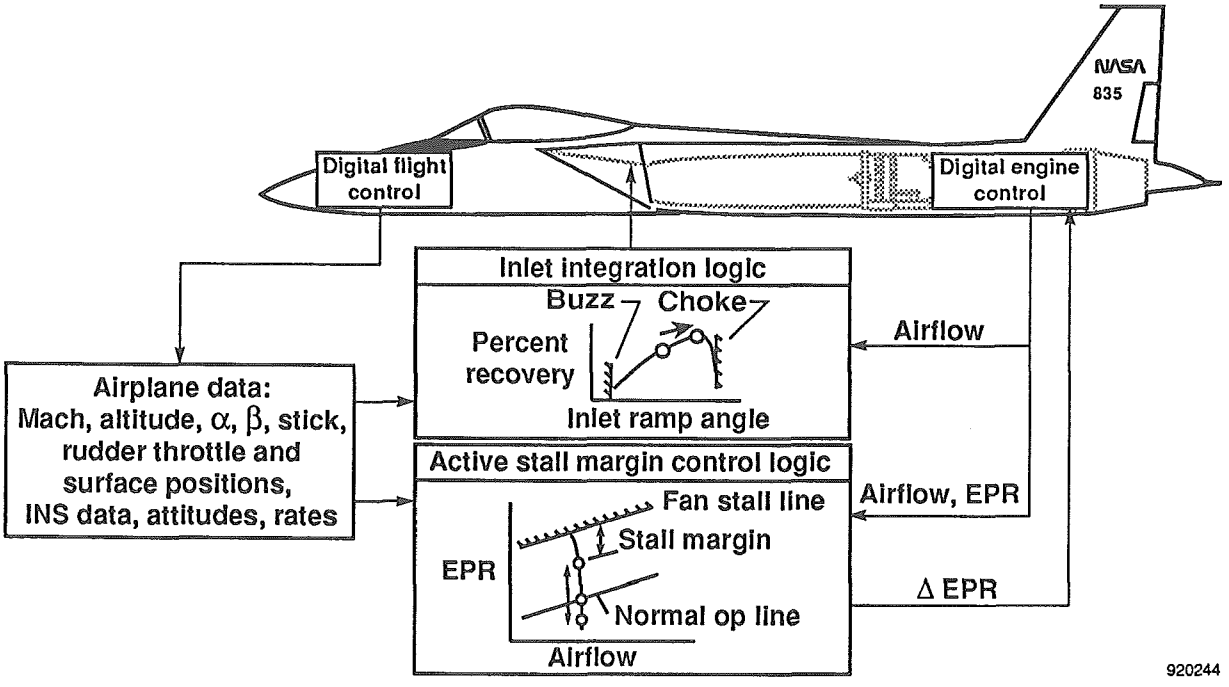

Figure 8. Engine-inlet-flight control integration.

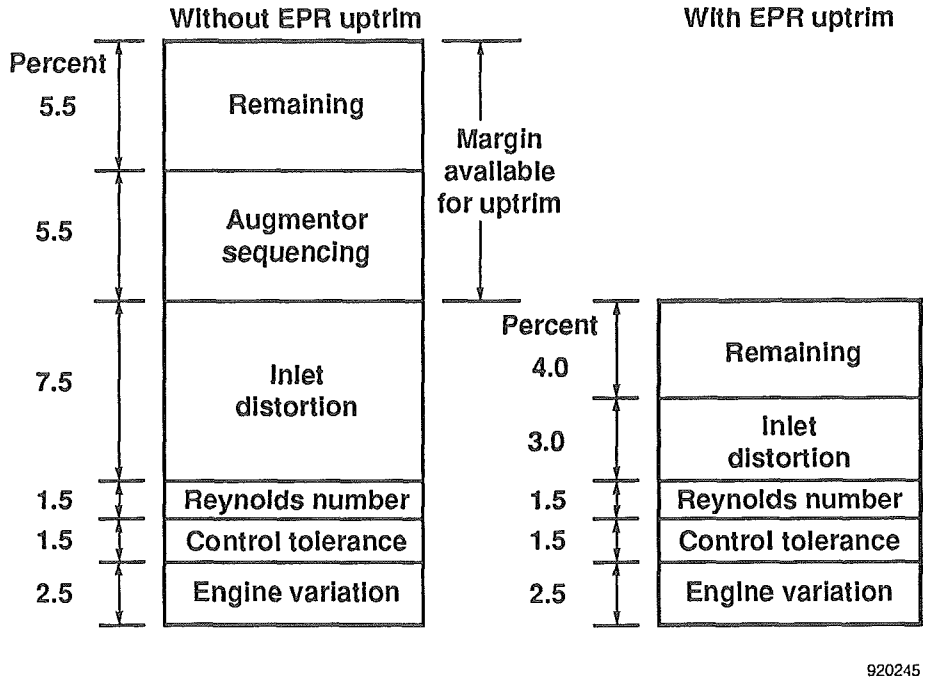

Figure 9. Stall margin available.

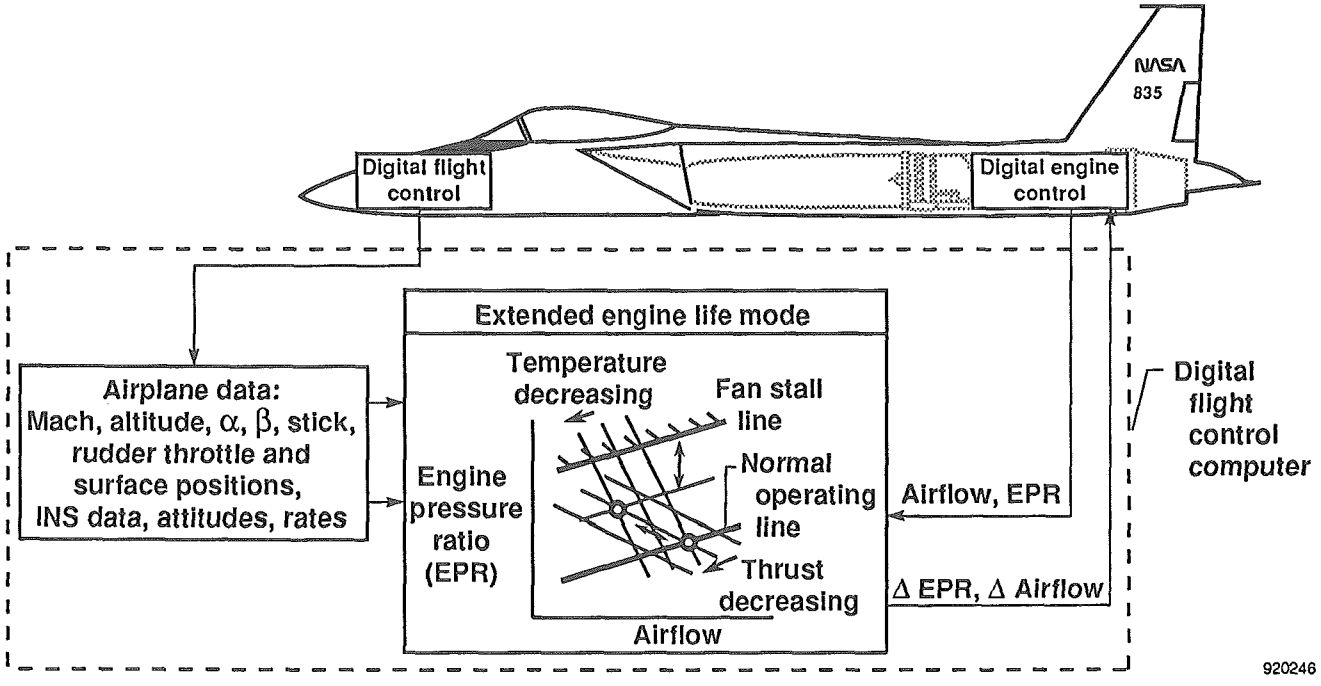

Figure 10. Extended engine life mode.

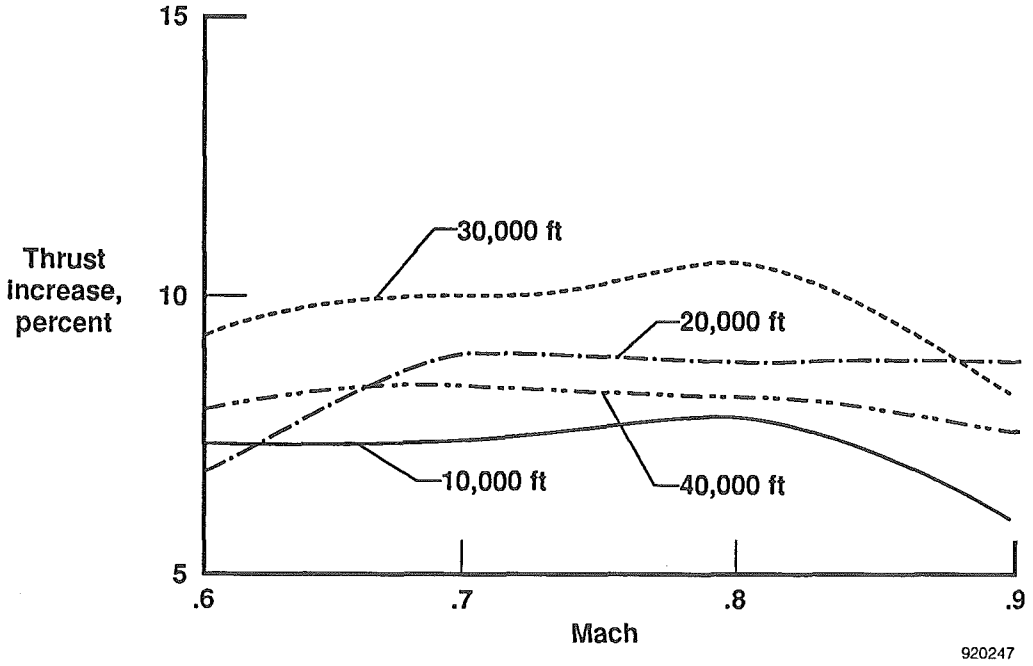

Figure 11. Engine pressure ratio mode.

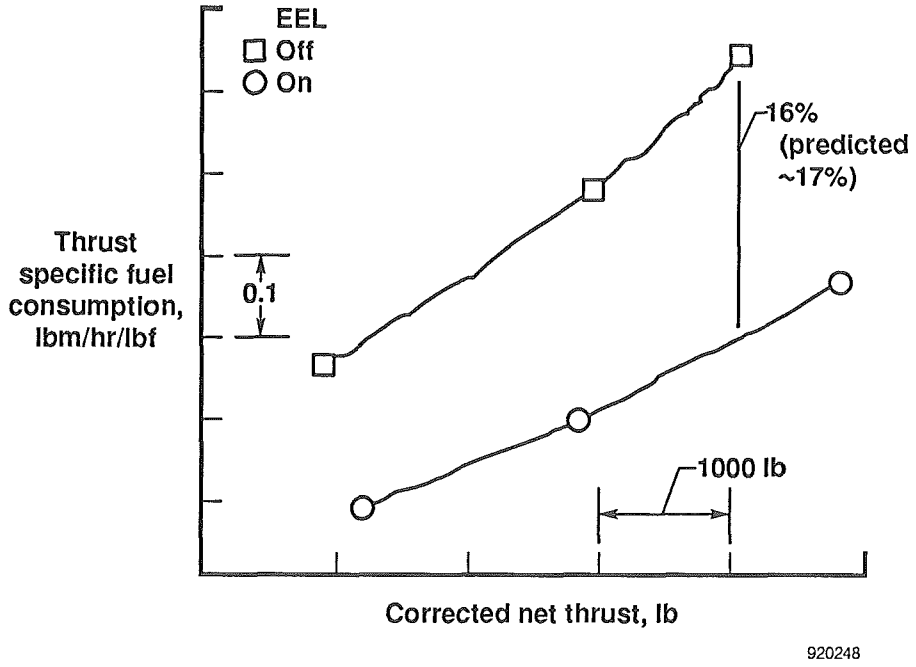

Figure 12. Percentage reduction in thrust-specific fuel consumption for afterburning power at Mach 0.6 and 30,000 ft, using advanced engine control system (EEL).

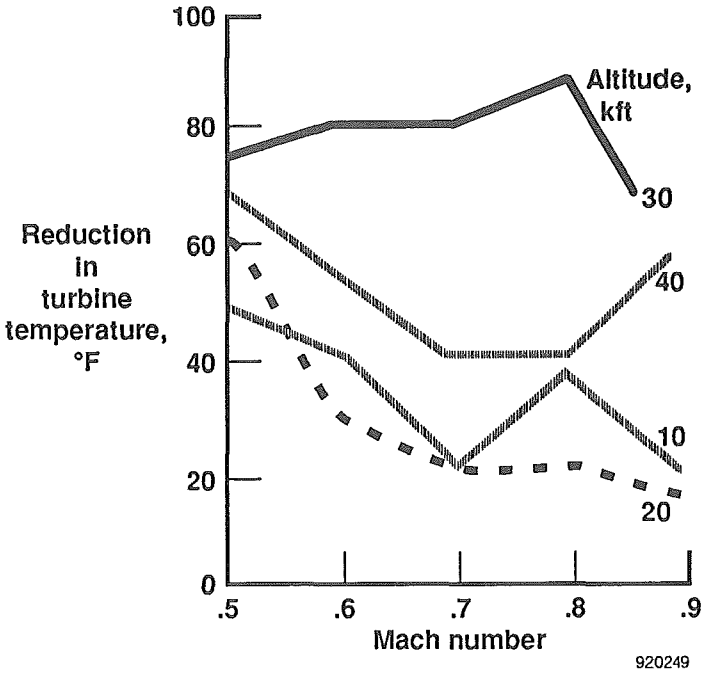

Figure 13. Results of extended-engine-life mode, military power.

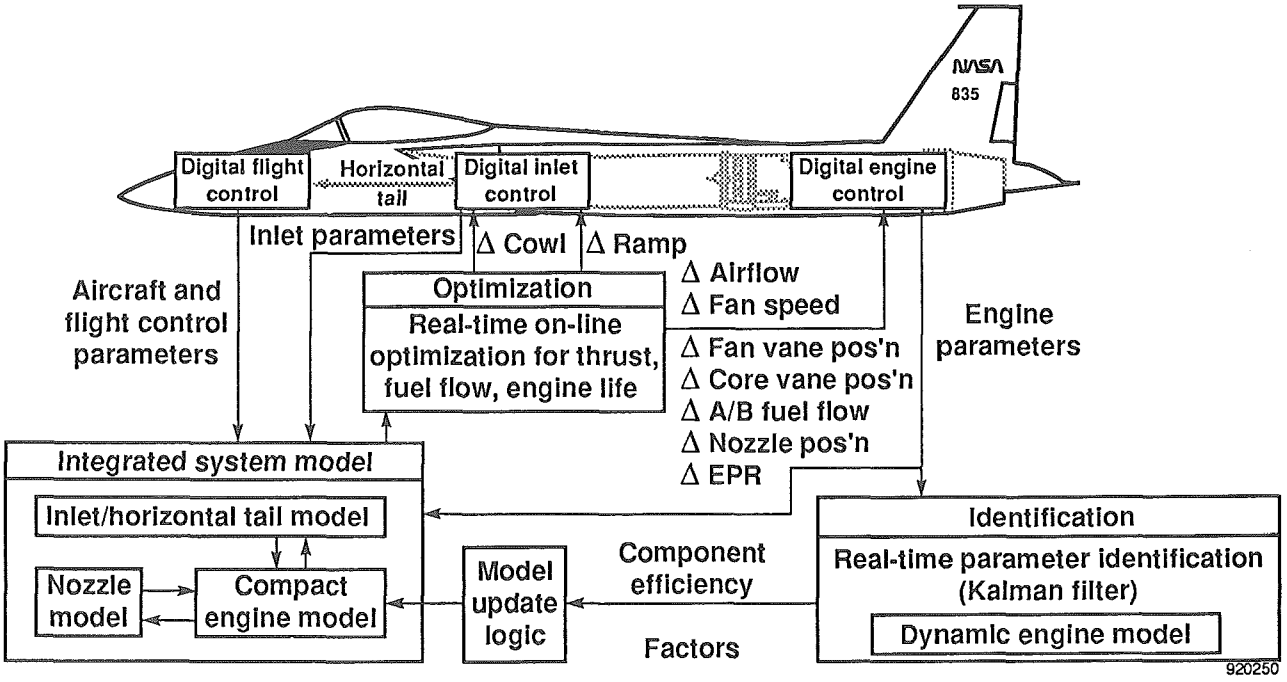

Figure 14. Performance seeking control for onboard, adaptive real-time optimization of performance.

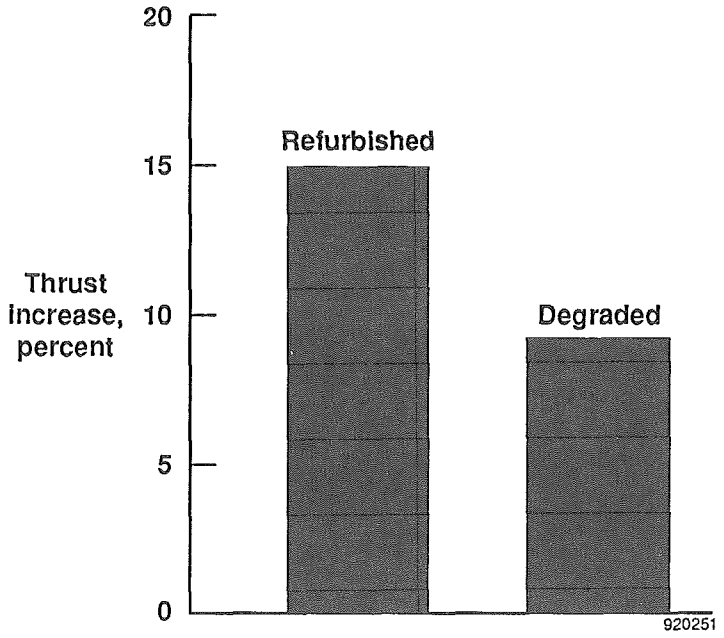

Figure 15. Maximum thrust mode results for performance seeking control (0.9 Mach, 15,000 ft, military power).

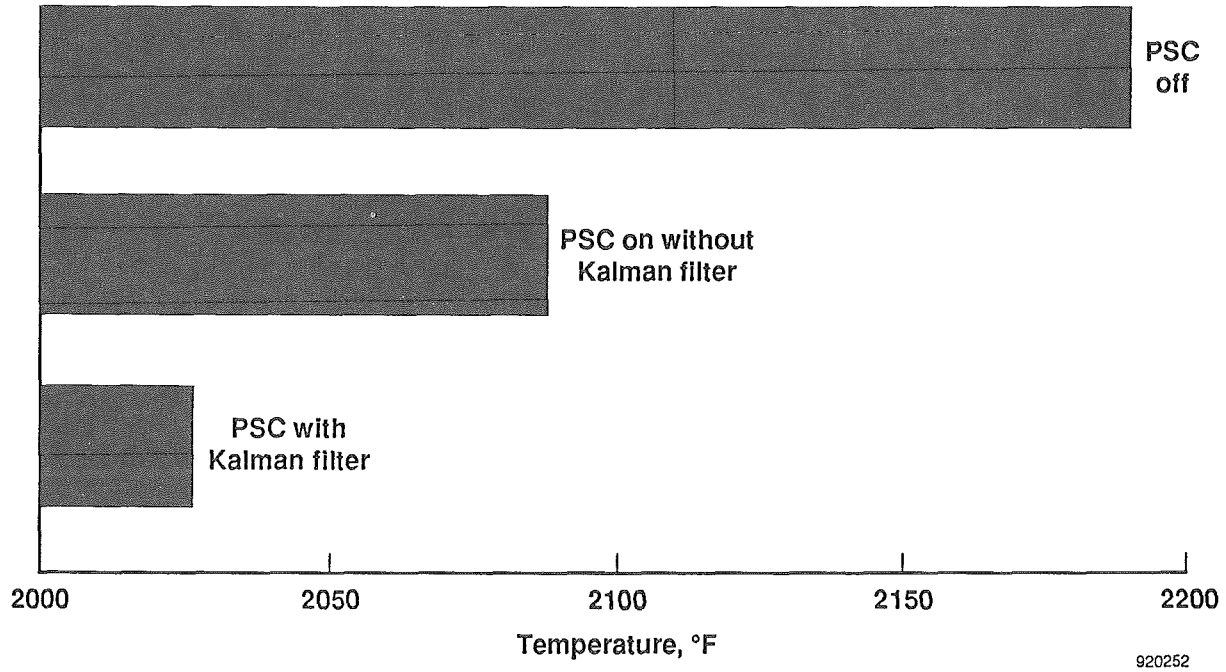

Figure 16. Extended engine life mode results for performance seeking control (0.9 Mach, 15,000 ft, military power, constant thrust).

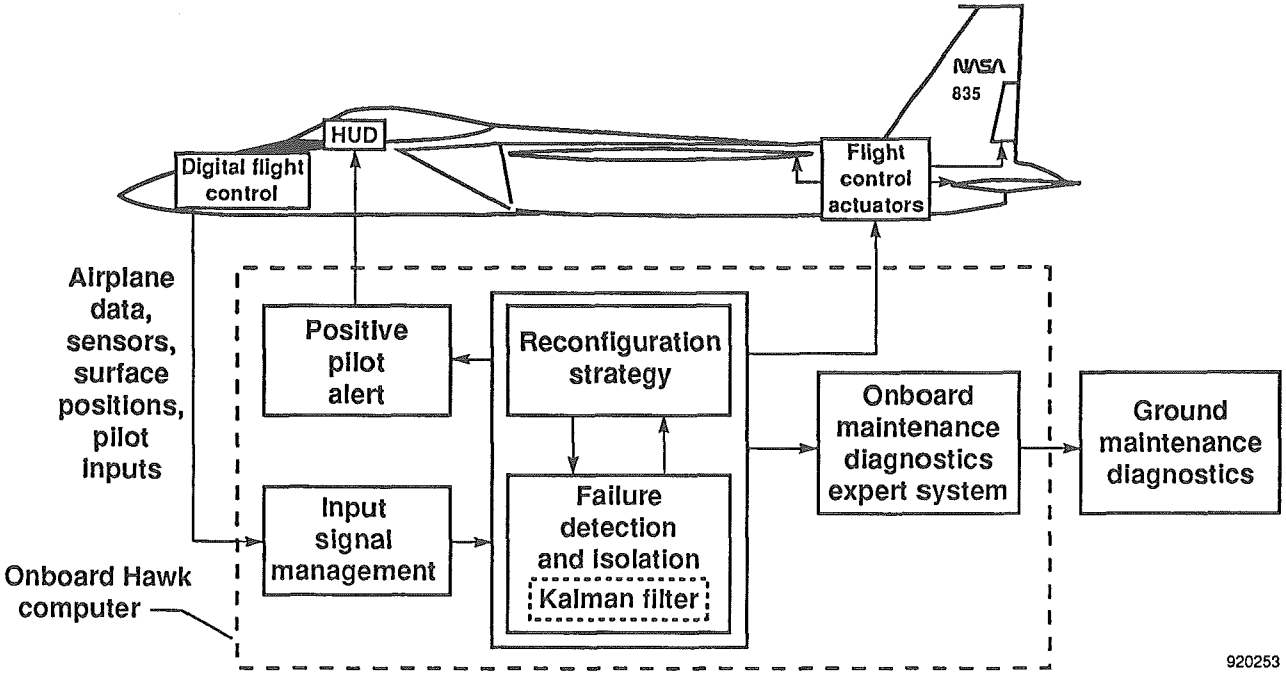

Figure 17. Self-repairing flight control system on F-15 aircraft.

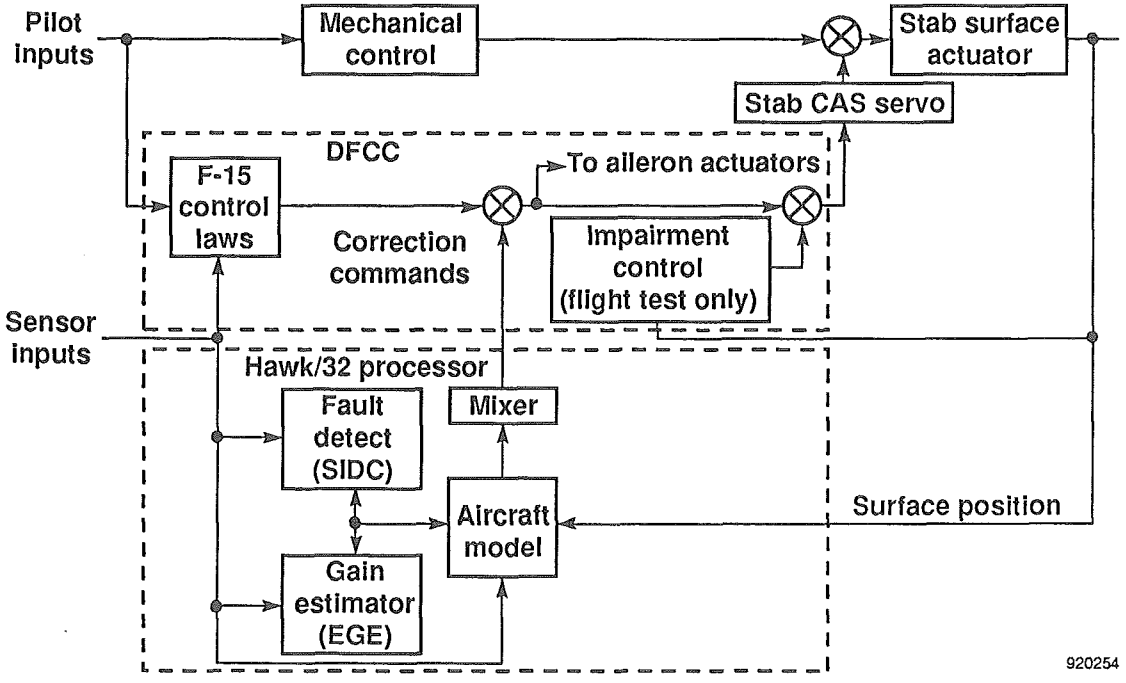

Figure 18. Implementation of self-repairing flight control system.

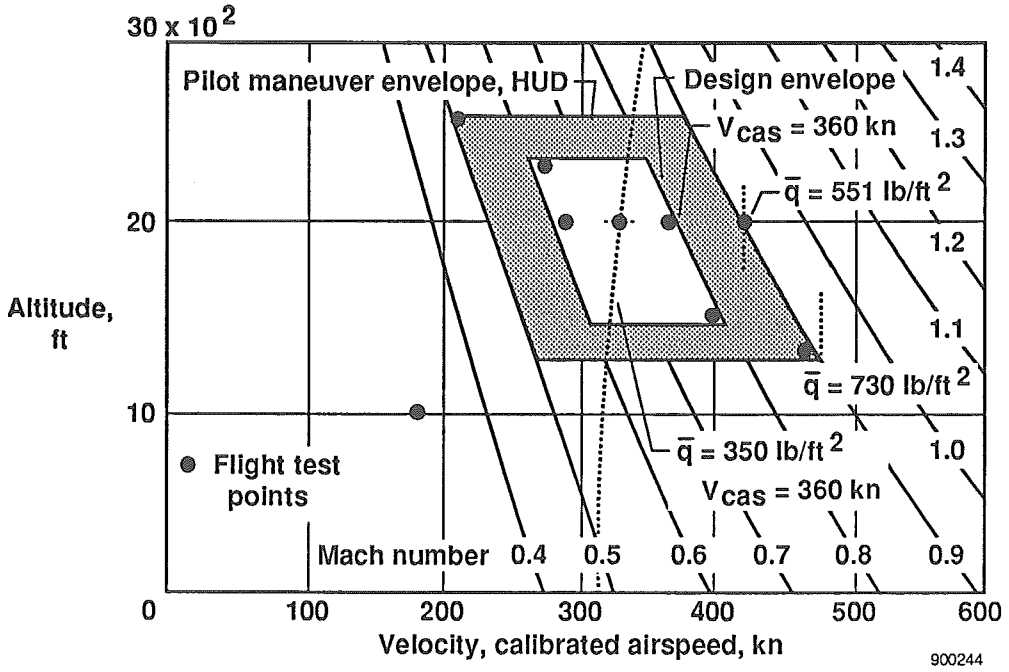

Figure 19. Flight demonstration test envelope for the F-15 SRFCS.

Fault scenario	Maneuver conditions	Failure indication major system	Subsystem failed	Cause
1	>3g	Roll CAS disengage	Dynamic pressure sensor	Connector fails under g load
2	1-g small pitch inputs	None	Stabilator surface	Actuator connecting pin
3	1-g small pitch inputs	Pitch, roll CAS disengage	Stabilator actuator	Hydraulic
4	2-g turn	Autopilot disengage	Inertial navigation system	Platform stabilization fails under g load
5	5-g turn	Pitch, roll CAS disengage	Pitch computer	Card A loose connection under g load
6	Pullup	CAS disengage	Right angle-of-attack sensor	Excessive friction in rotor

900245

Figure 20. In-flight maintenance diagnosis scenarios.

Fault detection, right stabilator partial missing

Correction detection and verification:	60 percent
Detection, no verification:	40 percent
False detection or verification:	0 percent

Fault detection, right stabilitor locked

Correct detection:	100 percent

Estimate of remaining stabilator surface

Correct value, span missing:	51 percent
(±20 percent tolerance)	

900246

Figure 21. Summary results of FDIE.

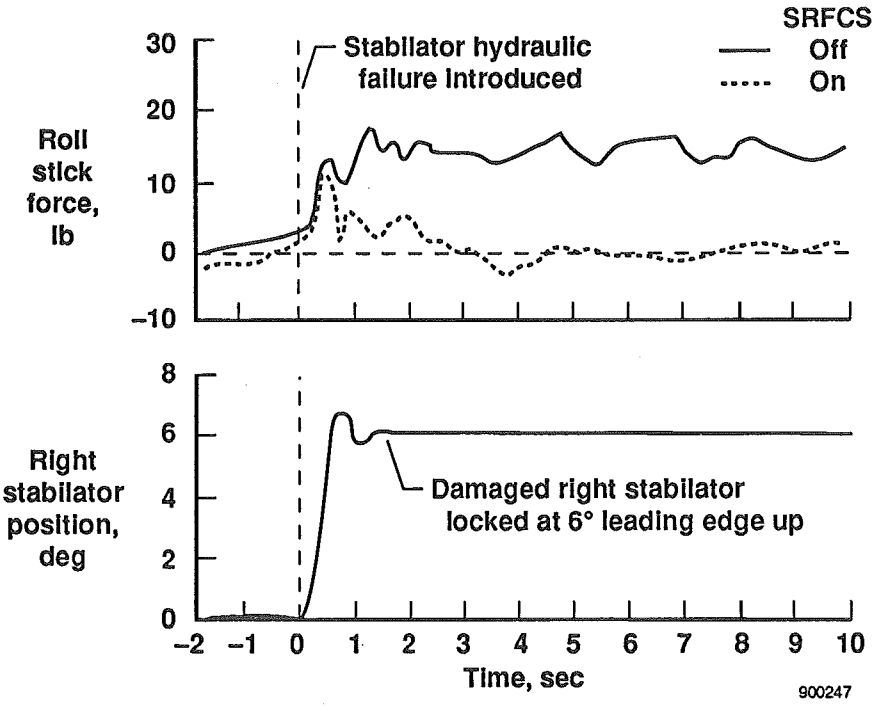

Figure 22. Flight data from F-15 SRFCS (Mach 0.7, altitude = 20,000 ft).

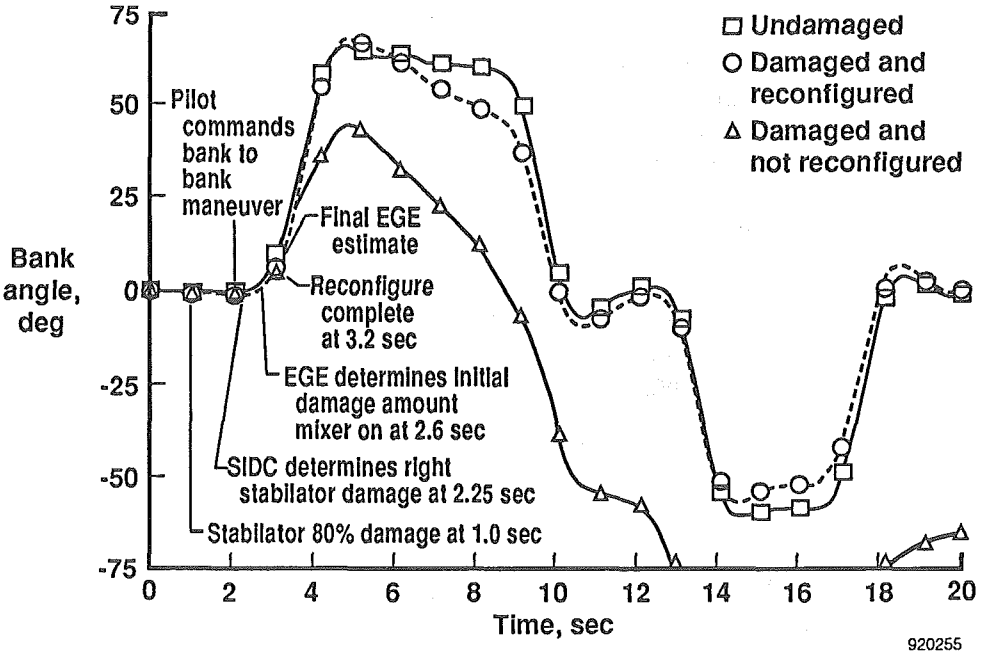

Figure 23. Bank response comparison for self-repairing flight control system.

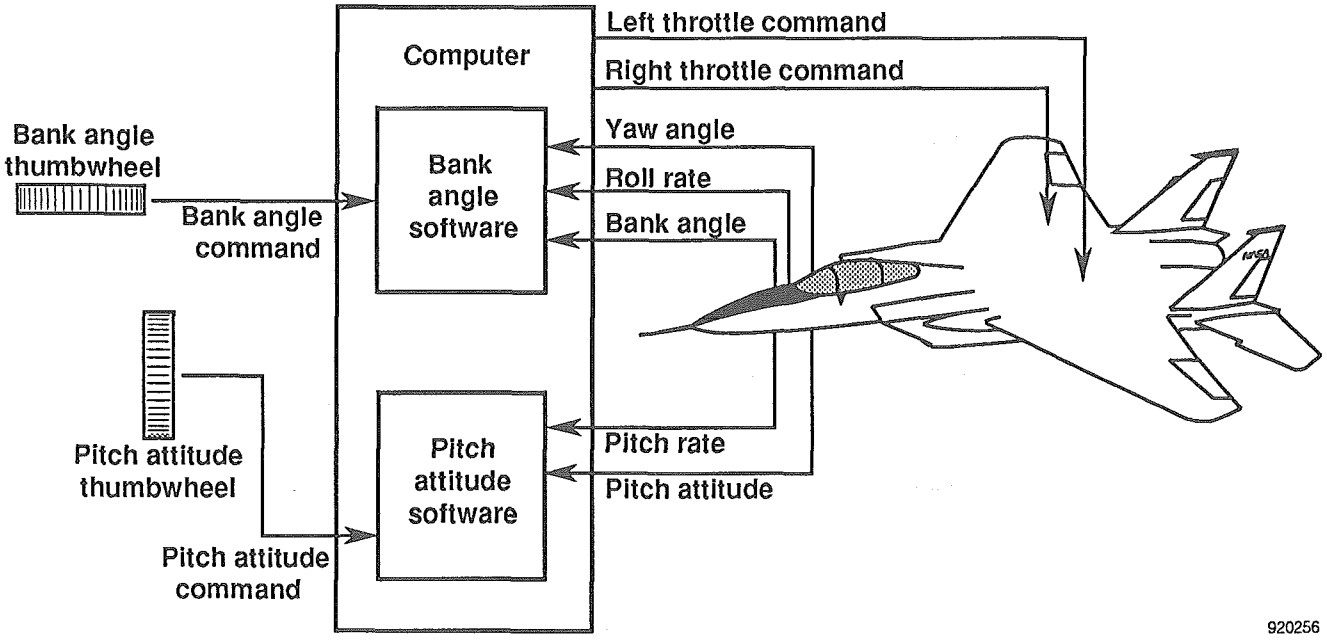

Figure 24. F-15 augmented throttles-only control system function.

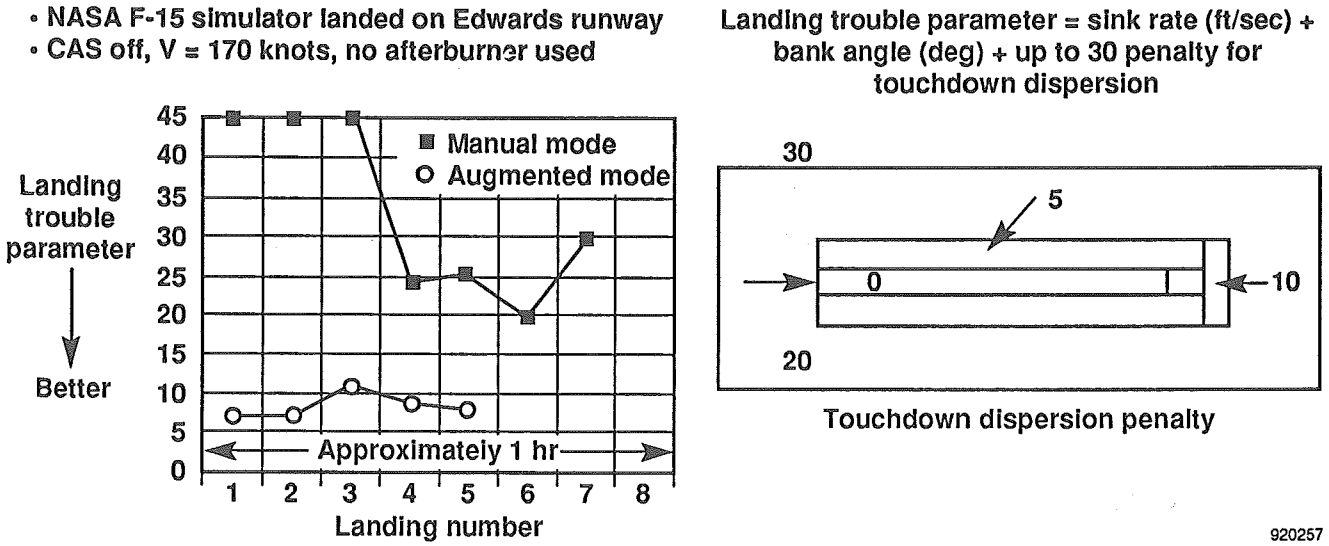

Figure 25. Results of PROTECT on the NASA F-15 aircraft.

ECN91 435-16

Figure 26. The thrust vectoring system installed on the HARV. A spin recovery parachute is mounted in the box between the upper vane actuator fairings.

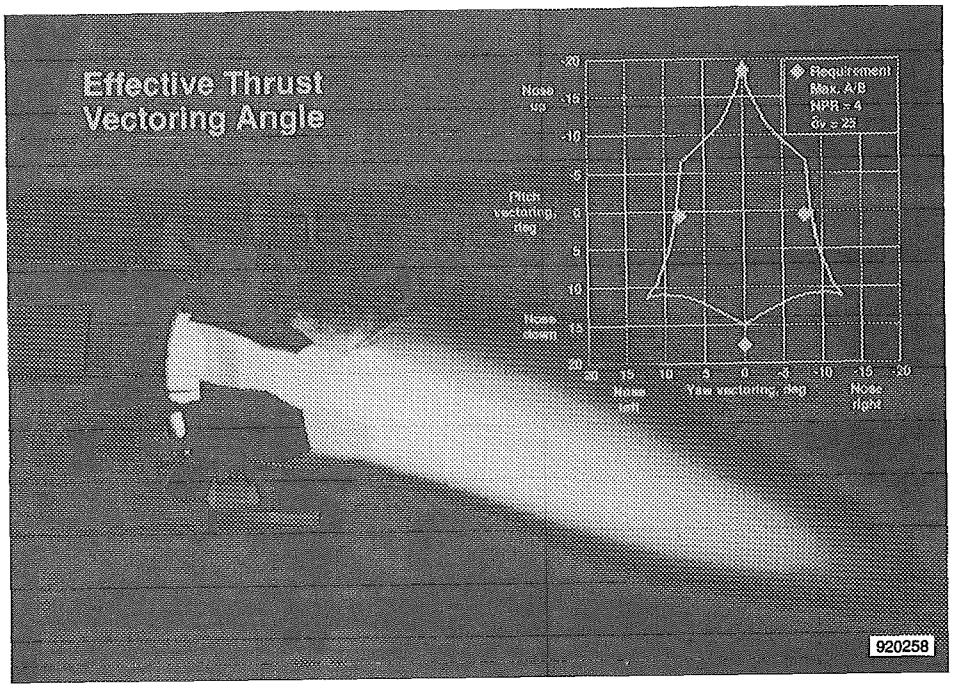

Figure 27. Predicted thrust-vectoring angle as a function of vane deflection.